

Flickering Events in Wind and Solar Power

Gerald Lohmann^{1,2}, M. Reza Rahimi Tabar¹, Patrick Milan¹, Mehrnaz Anvari¹,
Matthias Wächter¹, Elke Lorenz², Detlev Heinemann^{1,2}, Joachim Peinke¹

Abstract

This paper reports stochastic properties of renewable wind and solar energy resources by studying their conditional probability distribution functions (cpdf) in different time lags. The empirical results are obtained for data of global horizontal irradiance measured by a single sensor and the power output of a single wind turbine, as well as for an averaged solar sensor field and an aggregated wind farm. Moreover, the dependency of the time series' spread on the solar elevation angle, and the wind speed, respectively, is investigated in order to assess the risk of flickering in relation to these variables. The results show that the conditional distribution functions deviate strongly from Gaussian statistics and possess positive skewness, while the risk of flickering events in wind power and solar irradiance generally increases with wind speed and solar elevation, respectively, for single point measurements. Spatial averaging leads to flickering risk reduction.

1. Introduction

In the course of the decided exit from nuclear and fossil-fuel energy, German power grids face increasing challenges regarding the integration and management of wind and solar energy. As the shares of both renewable sources are on the rise, the guaranteed meeting of power demand and the maintenance of stability in voltage and frequency, amongst others, are expected to become more and more difficult due to the stochastic nature of wind speed and solar irradiance. Both resources are strongly intermittent in general and possess clusters of large amplitude fluctuations on short time scales [3, 6].

Wind turbulence is thereby responsible for the intermittency in wind power time series on short time scales, and the non-linear relation of wind speed u and wind power P (i.e. $P(t) \propto u^3(t)$) results in the power output of wind turbines being even more intermittent than wind speed itself. As for solar power in general and photovoltaics (PV) in particular, the dynamics of clouds and their size distributions are the origins of the intermittent characteristics of the respective time series. The on/off pattern of the rapid succession of direct sunlight exposure and cloud shadow coverage of a fixed location thereby leads to many extreme events of large amplitude ramps and jumps in solar irradiance [e.g. 9].

In [7] it is shown that the computed power spectrums from high frequency time series of global horizontal irradiance and wind power reveal a power-law behavior with an exponent $\sim -5/3$ (Kolmogorov exponent) in the frequency domain $0.001 \text{ Hz} < f < 0.5 \text{ Hz}$. This means that the power grid is essentially receiving input from turbulent-like sources. Although the spatial averaging acts as a filter [e.g. 1], strong deviations from Gaussian distributions remain the norm in the increment statistics of wind power and solar irradiance time series [6].

The uncontrollable fluctuations of these renewable sources in time are a major problem for keeping up the stability of power grids with high shares of wind and solar energy feed-in, especially regarding the high connection densities of photovoltaics in the distribution low-voltage grid [4, 8]. Therefore it is imperative to understand the nature of such fluctuations in order to successfully

¹ University of Oldenburg, 26111 Oldenburg, Germany, Institute of Physics, ForWind - Centre for Wind Energy Research

² University of Oldenburg, 26111 Oldenburg, Germany, Institute of Physics, Energy and Semiconductor Research Laboratory

manage decentralized power production, which is a main component in the exit from nuclear and fossil-fuel energy. Thus we investigate the non-Gaussian characteristics of solar and wind power time series in the following. We also study the occurrence and risk of flickering events with respect to different wind speeds and solar elevation angles for single point measurements and spatially averaged data.

2. Material and Methods

The results presented in this study are derived from data measured on operating wind turbines and continuous solar irradiance measurements with a sample rate of 1 Hz in Germany and Hawaii, respectively. The analyzed time series are the dimensionless wind turbines' scaled power output $P(t) = P_o(t)/P_r$, which is the quotient of the turbines' power output $P_o(t)$ and the turbines' rated power P_r , along with global horizontal irradiance $I(t)$ in units of Wm^{-2} . Figure 1 provides two typical subsets of the available data, illustrating the variations in time and the spatial smoothing effect of both the wind farm in relation to a single turbine (figure 1a), and the averaged global horizontal irradiance in a field in relation to a single sensor (figure 1b). The area containing the wind farm is about 4×4 km², while the solar field measures approximately 1×1 km².

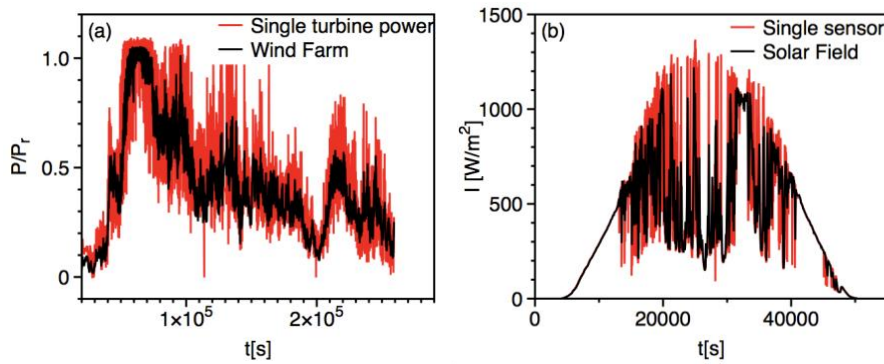


Figure 1: (a) Time series of normalized power output of a single wind turbine and the aggregated sum of a wind farm consisting of 12 turbines in an area of about 4×4 km². (b) Variations of the global horizontal irradiance measured by a single sensor and the averaged radiant flux density of 17 sensors in a solar field with an area of about 1 km².

Due to the different geographical origins of the used datasets, any comparison of the two must accept their respective meteorological conditions. While Hawaii is subject to tropical climate and trade winds, Germany is located in the temperate latitudes under the influence of prevailing westerlies. Both wind and solar energy resources are affected by the resultant differences to some extent, so it is important to keep in mind the different origins of the data.

As we aim to characterize the fluctuations in the aforementioned time series of wind power and solar irradiance, we compare their short time intermittency and extreme events using the estimation of their conditional probability distribution functions (cpdf) with short time lags in this study. We use the analysis of cpdfs in connection with a two dimensional contour plot. Stronger correlations between subsequent states in the time series thereby result in a more diagonal configuration in the two dimensional representation that facilitates the classification of cpdfs into their context.

Furthermore, we investigate the dependency of the time series' spread on certain conditions. In the case of wind power, the standard deviation

$$\sigma_u = \sqrt{\langle (P - \bar{P}(u))^2 | u \rangle}$$

of the scaled wind power P associated with different wind speeds u serves as an estimate of the stochasticity of wind power that is expected for different given wind speeds. Similarly, the standard deviation σ_α of the global horizontal irradiance I measured at different solar elevation angles α

$$\sigma_\alpha = \sqrt{\langle (I - \bar{I}(\alpha))^2 | \alpha \rangle}$$

expresses the influence of the apparent movement of the sun relative to Earth on the spread and the fluctuations in irradiance time series.

3. Results

When comparing the contour plot of wind power and solar irradiance, as well as some conditional pdfs for different values of power $P(t - \tau)$, with $\tau = 5$ s, and irradiance $I(t - \tau)$, with $\tau = 1$ s, fluctuations in the short time intervals τ and non-Gaussian characteristics of the associated cpdfs are evident for both renewable energy sources (see figure 2). The left panels of figure 2 thereby provide an overview of the short term correlations in wind power and irradiance time series by means of the contour plots of $P(t)$ vs $P(t - \tau)$ in the upper panel, and $I(t)$ vs $I(t - \tau)$ in the lower panel, respectively. For three certain transects $\alpha_1, \alpha_2, \alpha_3$ of $P(t - \tau)$ and $I(t - \tau)$, respectively, the corresponding conditional pdfs are plotted in the right panels. Gaussian distributions are also provided for comparison.

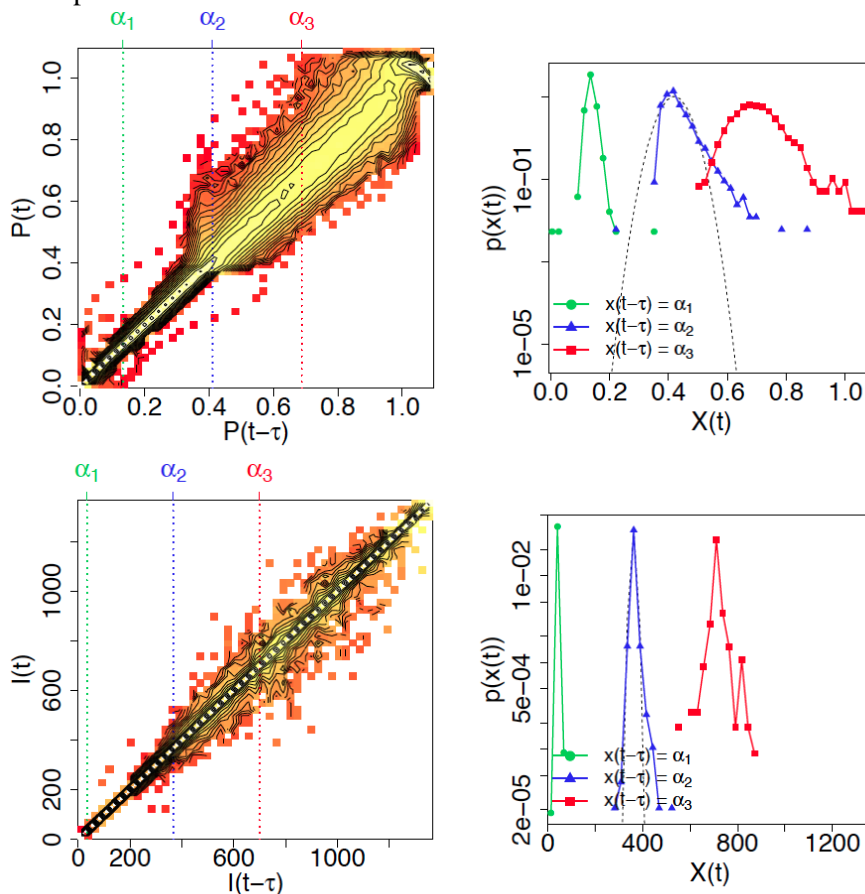


Figure 2: The panels show the contour plots (left) and conditional pdfs (right) of wind power for a single turbine with a time lag of $\tau = 5$ s (top), and of global horizontal irradiance for a single sensor with a time lag of $\tau = 1$ s (bottom).

As for the wind power analysis in the top panels of figure 2, lower magnitude subsets of the time series $P(t - \tau) < 0.4$ are mostly correlated strongly with their subsequent $P(t)$, which is demonstrated by a low spread and close adherence to the diagonal line ($y = x$) in the contour plot, as well as a very narrow conditional pdf of the transect at α_1 . In contrast, the contour plot of wind

power begins to exhibit weaker correlations of subsequent states at $P(t - \tau) \approx 0.4$, and continues to prove weakly correlated characteristics for all higher magnitudes of wind power $P(t - \tau) > 0.4$. The positive skewness of the conditional pdfs at α_2 and α_3 show that higher values of $P(t)$ are more likely to follow $P(t - \tau)$ than lower ones. The fat-tailed structures of the cpdfs indicate the possibilities of large magnitude fluctuations of power in short time scales, which is considered flickering in the time series.

The analysis of the bottom panels of figure 2 reveals similar general characteristics for global horizontal irradiance as previously identified for wind power, while some differences are also present. Both low and high magnitude subsets of the time series $I(t - \tau) < 200 \text{ Wm}^{-2}$ and $I(t - \tau) > 1200 \text{ Wm}^{-2}$ are shown to be mostly correlated strongly with their following $I(t)$, as there is a low spread and a close adherence to the diagonal line ($y = x$) in the contour plot. Consequently, the conditional pdf of the transect at α_1 is very narrow. In between the two aforementioned values, the time series is only weakly correlated to its previous state, with most flickering events occurring around $I(t - \tau) \approx 850 \text{ Wm}^{-2}$, as illustrated by the spread of the contour plot. Both positive skewness and fat tails of the conditional pdfs at α_2 and α_3 are less pronounced compared to wind power, but still evident.

The dependency of flickering in wind power and solar irradiance on wind speed and solar elevation angle, respectively, may be analyzed by means of figure 3. The standard deviation σ_u of wind power associated with certain wind speeds is visualized for a single turbine and the aggregated sum of the wind farm in figure 3a, while the standard deviation σ_α of global horizontal irradiance associated with certain solar elevation angles is displayed in figure 3b.

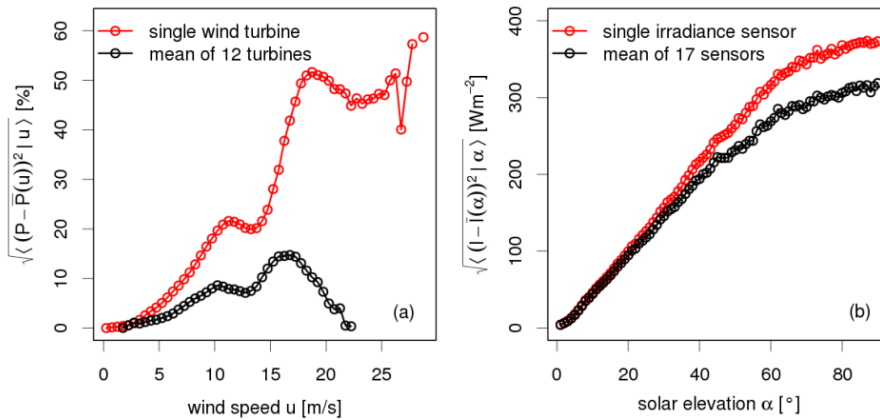


Figure 3: (a) The standard deviation of the normalized wind power output, conditioned to the wind speed, and (b) the standard deviation of global horizontal irradiance, conditioned to the solar elevation angle

In case of the wind power, both single turbine and wind farm exhibit increasing values of standard deviation σ_u of conditioned wind power time series with increasing wind speeds until a local maximum around $u \approx 11 \text{ ms}^{-1}$, and $u \approx 10 \text{ ms}^{-1}$, respectively. A significant increase of σ_u is further evident for the single turbine, while σ_u of the wind farm output increases at a much smaller rate until it reaches a global maximum around $u \approx 16 \text{ ms}^{-1}$, after which it decreases sharply. The single wind turbine power spread exhibits a similar maximum around $u \approx 18 \text{ ms}^{-1}$, but there are both higher and lower σ_u present for even higher wind speeds $u > 18 \text{ ms}^{-1}$. Spatial smoothing obviously has a big impact on the difference of the two curves and suggest much more flickering in the output of a single wind turbine compared to the output of a wind farm. Please note that there are no wind farm power outputs associated with high wind speeds $u > 22 \text{ ms}^{-1}$, because wind

turbulence is also affected by spatial averaging, of course, and the highest wind speed values measured at a single turbine never occur in the entire wind farm simultaneously.

The characteristics of the standard deviation σ_α of solar irradiance conditioned to solar elevation angle α are different, as σ_α keeps increasing rather smoothly with increasing α for both a single sensor and the mean of the solar field. However, spatial smoothing effects are also evident to a lesser extent, and for solar elevation angles above $\alpha > 30^\circ$.

4. Discussion

The results presented in the previous section confirm the flickering attributes of wind and solar power by showing the weak correlation of subsequent states in the analyzed time series and the non-Gaussian characteristics of corresponding conditional pdfs.

In this regard, it is especially interesting to note the strongly positive skewness of the cpdf α_2 in the upper panels of figure 2. For the order of wind power $P(t - \tau) \approx 0.4$, it shows that the subsequent power value $P(t)$ is very likely to be much higher than its predecessor but comparatively unlikely to be lower. We relate this phenomenon to the effect of inertia in a rotating wind turbine: when a wind gust hits the blades, the power is immediately increased by the exercised torque, while the power will not drop within the same timeframe if the wind speed decreases for a moment, because the inertia of the rotating generator. This argumentation also qualitatively explains the positive skewness of cpdf α_2 in the upper panels of figure 2. The decrease in magnitude of this effect from cpdf α_2 to cpdf α_3 may be connected with some specifications of the wind turbine and possibly results from internal control mechanisms or some other turbine properties that exhibit different effects at different levels of power output.

The fact that both positive skewness and fat tails of the conditional pdfs are less pronounced in the case of solar irradiance (bottom panels of figure 2) compared to wind power (top panels of figure 2), may be attributed to the different values of $\tau = 5$ s for wind power and $\tau = 1$ s for solar power. We confidently expect the non-Gaussian characteristics of global horizontal irradiance to be more pronounced for increasing τ , as reported by [6].

As for the positive skewness of conditional pdfs for solar irradiance, we refer to the typical diurnal variation of global horizontal irradiance in Hawaii: after sunrise, the skies are usually clear and global horizontal irradiance increases with the solar elevation angle until sometime in the morning, when strong convection leads to the formation of cumulus-type clouds that cause measured irradiance to flicker strongly due to the cloud shadows passing rapidly over the ground. More often than not, this cloud behavior dominates during the rest of the day, so that there are more afternoons with flickering events than mornings. This asymmetry in the diurnal variation of solar irradiance in Hawaii may be related to the slight positive skewness of the cpdfs as observed in figure 2.

The well pronounced dependency of the standard deviation σ_α of solar irradiance on the solar elevation angle, and the more pronounced spatial smoothing of wind power variability illustrated in figure 3 give rise to the following remarks. Essentially, the former relationship illustrates the simple fact that the maximum possible radiant flux density of solar irradiance is higher for large solar elevation angles than for low ones. The fluctuations in irradiance reflected in the standard deviation of the time series are thus bound in magnitude to the maximum possible irradiance. This means that similar cloud dynamics will, of course, result in different irradiance fluctuations, depending on the solar elevation angle. In terms of wind power standard deviation σ_u and wind speed, there is a profoundly different relationship in the spatial smoothing on small scales: while there is no spatial variability in the solar elevation angle, wind speeds are highly variable. Thus, the different wind turbines are subject to different wind speeds at the same time, but the different solar sensors are always exposed to the same solar elevation angle simultaneously.

5. Conclusion

In this contribution we study flickering events in wind power and solar irradiance time series and show that their conditional pdfs exhibit fat-tailed non-Gaussian characteristics with positive skewness. Moreover, we find that the risk of flickering in wind power increases with the wind speed for a single turbine, while the effect of spatial smoothing leads to a significant flickering risk reduction for high wind speeds in a wind farm. Similarly, the risk of high magnitude flickering in solar irradiance steadily increases with the solar elevation angle, because the higher the solar elevation, the more radiant flux density is available in global horizontal irradiance.

To continue our work, the next steps will include the development and evaluation of possible methods to suppress the flickering events based on power electronics and their control strategies, as well as the consideration of possible PV-related system characteristics that may affect the conversion of flickering in irradiance to flickering in PV system power output, like reported by [2]. Furthermore, we strive to acquire high resolution wind and solar measurements from the same location in order to analyze possible correlations in their respective fluctuation characteristics.

Finally classifying wind and solar power resources in terms of their stochastic properties will contribute to operating micro grids and virtual power plants reliably with high shares of renewables, as the quality of their respective control strategies and products are strongly influenced by flickering in power input. Generally, conditions of low flickering probabilities will allow more flexible network designs in both micro grids and virtual power plants, while conditions of high flickering call for larger aggregations of networks to balance the expected fluctuations.

Acknowledgements

The Lower Saxony research network “Smart Nord” acknowledges the support of the Lower Saxony Ministry of Science and Culture through the “Niedersächsisches Vorab” grant programme (grant ZN 2764/ZN 2896). We acknowledge also the National Renewable Energy Laboratory of the United States for providing the global horizontal irradiance data in Hawaii [5], and Deutsche Windtechnik AG Bremen for providing us with measurement data from the wind turbines.

References

- [1] M. Lave, J. Kleissl, and E. Arias-Castro, “High-frequency irradiance fluctuations and geographic smoothing,” *Solar Energy*, vol. 86, no. 8, pp. 2190–2199, 2012.
- [2] J. Marcos, L. Marroyo, E. Lorenzo, D. Alvira, and E. Izco, “From irradiance to output power fluctuations: the PV plant as a low pass filter,” *Progress in Photovoltaics: Research and Applications*, vol. 19, no. 5, pp. 505–510, 2011.
- [3] P. Milan, M. Wächter, and J. Peinke, “Turbulent Character of Wind Energy,” *Physical review letters*, vol. 110, no. 13, p. 138701, 2013.
- [4] O. Perpiñán, J. Marcos, and E. Lorenzo, “Electrical power fluctuations in a network of DC/AC inverters in a large PV plant: Relationship between correlation, distance and time scale,” *Solar Energy*, vol. 88, no. 0, pp. 227–241, Feb. 2013.
- [5] M. Sengupta and A. Andreas, *Oahu Solar Measurement Grid (1-Year Archive): 1-Second Solar Irradiance; Oahu, Hawaii (Data)*. 2010. doi:10.7799/1052451
- [6] M. R. R. Tabar, M. Anvari, M. Wächter, P. Milan, G. Lohmann, E. Lorenz, D. Heinemann, J. Peinke, “Renewable Power from Wind and Solar: Their Resilience and Extreme Events,” submitted.
- [7] M. R. R. Tabar, M. Anvari, G. Lohmann, D. Heinemann, M. Wächter, P. Milan, E. Lorenz, and J. Peinke, “Kolmogorov spectrum of renewable wind and solar power fluctuations,” *Eur. Phys. J. Spec. Top.*, vol. 223, no. 9, pp. 1–8, Jul. 2014.
- [8] A. Woyte, V. Van Thong, R. Belmans, and J. Nijs, “Voltage fluctuations on distribution level introduced by photovoltaic systems,” *Energy Conversion, IEEE Transactions on*, vol. 21, no. 1, pp. 202–209, 2006.
- [9] A. Woyte, R. Belmans, and J. Nijs, “Fluctuations in instantaneous clearness index: Analysis and statistics,” *Solar Energy*, vol. 81, no. 2, pp. 195–206, 2007.